$E1$ and $M1$ strength functions from average resonance capture data

J. Kopecky,[1] S. Goriely,[2] S. Péru,[3] S. Hilaire,[3] and M. Martini[4]
[1]*JUKO Research, Kalmanstraat 4, 1817 HX Alkmaar, The Netherlands*
[2]*Institut d'Astronomie et d'Astrophysique, Université Libre de Bruxelles, CP-226, 1050 Brussels, Belgium*
[3]*CEA, DAM, DIF, F-91297, Arpajon, France*
[4]*ESNT, CEA, IRFU, Service de Physique Nucléaire, Université de Paris-Saclay, F-91191, Gif-sur-Yvette, France*
(Received 22 September 2016; revised manuscript received 24 March 2017; published 22 May 2017)

The average resonance capture (ARC) data measured at different filter beam facilities are re-analyzed. They include all measurements made between 1970 and 1990, but only partially exploited. Updated spectroscopic information on the states of interest as well as on s-wave resonance spacing are used to extract the $E1$ and $M1$ photon strength function. This re-evaluation aims at providing experimental information on the $E1$ and $M1$ strength function around the neutron binding energy and in doing so provides also constraints for existing models used in statistical reaction codes. The revised data are compared to the photon strength function extracted from other experimental methods, such as photoneutron data and Oslo-method data. We also compare the ARC data with recent quasiparticle random phase approximation calculations based on the D1M Gogny force. The ratio of the $E1$ to $M1$ strength functions is also analyzed and proposed as a new stringent test for the future elaboration of theoretical models for the dipole strength function.

DOI: 10.1103/PhysRevC.95.054317

I. INTRODUCTION

Photonuclear and neutron capture data, describing interactions of photons and neutrons with atomic nuclei, are of importance for a variety of applications such as (i) radiation shielding and radiation transport analyses (in particular, for the production of photoneutrons with energies above 8 MeV), (ii) the calculation of an absorbed dose in the human body during radiotherapy, (iii) activation analyses, safeguards, and inspection technologies (identification of materials through radiation induced by photonuclear reactions using portable bremsstrahlung devices), (iv) nuclear waste transmutation, (v) fission and fusion reactor technologies, and (vi) astrophysical processes of nucleosynthesis. Photon strength functions (PSF) describe the average response of the nucleus to an electromagnetic probe, and are thus a fundamental quantity of interest for the modeling of nuclear reactions, and more particularly radiative captures. In the past two decades, there has been considerable growth in the amount of reaction data measured to determine integrated photon strength functions. These include various experimental techniques, such as photon scattering based on mono-energetic or bremsstrahlung photon sources [1,2], charge-particle reactions (such as those used in the Oslo method) [3], neutron capture reactions [4], and photoabsorptions [5,6]. For more details, the reader is referred to the review [7].

In addition to these experimental techniques, the average resonance capture (ARC) data measured at filter beam facilities can be used to provide information on the PSF and its various multipolarities. Such measurements have been essentially conducted at Argonne National Laboratory (ANL) [8], Idaho Nuclear Engineering Laboratory (INEL) [9], Kiev [10], and Brookhaven National Laboratory (BNL) [11] laboratories during the period between 1970 and 1990, but rarely exploited to obtain PSF information. The accent of these measurements was given to the spectroscopy of low-lying final states [12,13] and only a limited number of publications presented the measured data as the PSF results [14–17].

The main aim of this work was to recover old ARC measurements, select the best ones, and convert them into PSF to enable their use in the verification of different strength function models. Since the original period of ARC measurements, more or new spectroscopic information on the final states of interest have been obtained; similarly more accurate determinations of the s-wave resonance spacing are available and can consequently improve the extraction of the PSF from ARC measurements.

Quite often the different experimental techniques lead to discrepant results and users are faced with the dilemma of trying to decide which (if any) amongst the divergent data they should adopt.

The paper is organized as follows. In Sec. II, the ARC data, which includes a selection of recommended data from available measurements, are presented with the conversion of the data into a strength function. A detailed description of the uncertainties affecting such data is also presented in this section. In Sec. III, the ARC $E1$ and $M1$ strength functions are compared to the recent model based on the axially-symmetric-deformed HFB + QRPA calculation. Conclusions are finally drawn in Sec. IV.

II. ARC ATLAS

The principles of resonance-averaged capture have been thoroughly reviewed in Refs. [12,18,19]. ARC data are typically produced by transmission through different materials such as boron, ^{45}Sc (2 keV) or ^{56}Fe (24 keV) filters that yield bell-shaped beams from transmission dips of a few keV wide. The boron-filtered beam primarily filters out the thermal capture component. The ARC neutron energy range is small enough, so that primary γ-ray widths are only slightly broadened leading to a possible analysis of the discrete γ-ray transitions. The resonance averaging is a direct way to study the energy variation of $E1$, $M1$, and $E2$ strength, as long

as the averaging sufficiently smooth out the Porter Thomas fluctuations of transition probabilities. ARC measurements provide primary γ-ray relative intensities in arbitrary units that need to be converted into transition probabilities by normalizing the transition probabilities to low-lying states to that observed in discrete resonance neutron capture (DRC). ARC data are usually dominated by the s-wave capture, but for 2 keV and even more 24 keV neutrons a possible nonnegligible contribution from the p-wave capture has to be taken into account.

We reanalyzed all the available (to us) ARC data measured at different filter beam facilities. The list of data sources used in this re-evaluation is given in Table I. It includes all measurements, which have been recovered from the period after 1970. Corresponding references are quoted. Some of the data processed in the former collaboration between BNL (Chrien) and ECN (Kopecky) are referred to as BNL/ECN database and includes some published and unpublished BNL data. The original idea of this data base was to form a complete starter file of ARC measurements to be used for PSF data, however, it was not completed at that time. It includes entries for about 15 nuclides of B- and Sc-filter measurements and its I_γ/E_γ^3 file has been processed with the SPARC and RACA codes [20,21].

The primary gamma rays from ARC experiments are given as the reduced intensities by the phase factor for dipole radiation I_γ/E_γ^3 in arbitrary units. Their multipolarity is deduced from the spin or parity assignments of the corresponding final states. For more details about the ARC analysis, we refer the reader to Refs. [12,15,18,19]. The present re-evaluation includes some revisions of the γ-ray multipolarity, using the recent spectroscopic information of the final states from the IAEA-NDS ENDF library and the update of resonance spacing D_0 [22,23]. The boron and 2-keV spectra are always chosen for PSF evaluation, because of their superior statistical quality and of the negligible or smaller effect from p-wave capture contamination.

A. Conversion of data into $f(L)$ scale

The applied revision resulted in a data set of reduced relative intensities, consisting of three well-separated intensity groups. They belong to three multipolarity modes, namely $E1$, $M1$, and often also $E2$ transitions, respectively. The broadness of these groups is primarily due to the statistical and Porter-Thomas (PT) fluctuations and reflects the quality of averaging. The conversion of I_γ/E_γ^3 values into the γ-ray strength function scale $f(L)$ in 10^{-8} MeV^{-3} units has still to be applied (see, e.g., Ref. [15]). Because the initial state is a mixture of a number of many initial states (resonances) in the filtered beam profile and cannot be uniquely defined, some external information has to be used. The DRC is the best source for such information, it is the same physical process at a similar neutron energy. The initial states, the resonances, have well-defined orbital momentum and parity parameters.

First, the dependence of averaged intensities I_γ/E_γ^3 on the spin of the final state has to be removed. This is based on the different population of the J_f final spin groups from the initial target spin with $J_t \pm 1/2$ and $J_t \pm 3/2$ values. For data adopted in the BNL/ECN source, the analysis using the SPARC and RACA codes [20,21] was adopted. In case such an analysis is

TABLE I. List of recovered ARC measurements with neutron filtered beams (B, Sc, or Fe). The x symbols shows that the data are included in the ARC Atlas starter database.

Nuclide	B	Sc	Fe	Ref.
As-96		x	x	[24]
Mo-96		x	x	BNL/ECN, [25]
Mo-98		x	x	[25]
Ru-102		x	x	BNL/ECN
Pd-106	x	x	x	[8,15,26,27], BNL/ECN
Cd-114		x	x	BNL/ECN, [28]
Te-124		x	x	[29]
I-128		x		[27]
Ba-135		x	x	[30]
Ba-136		x	x	[31]
Nd-146	x	x		[32,33]
Sm-155		x	x	[34], BNL/ECN
Eu-154		x	x	[35]
Gd-155		x	x	[36–38]
Gd-156	x	x		[8,17,38,39]
Gd-157		x	x	[37], BNL/ECN
Gd-158	x	x	x	[8,40,41]
Gd-159		x	x	[38,42]
Dy-162		x	x	[43], BNL/ECN
Dy-163		x	x	[44]
Dy-164		x	x	[43], BNL/ECN
Dy-165		x	x	[45]
Ho-166	x			[8]
Er-168	x	x	x	[8,46], BNL/ECN
Tm-170		x	x	[47]
Yb-172		x	x	[48], BNL/ECN
Yb-174		x	x	[49,50]
Lu-176		x	x	[51], BLN/ECN
Hf-178		x	x	[52]
Ta-182		x		[53]
W-184	x	x		[9,54]
W-185		x	x	[55]
W-187		x	x	[55]
Os-188		x	x	[10]
Os-189		x	x	[56]
Os-191		x	x	[57]
Os-193		x	x	[58]
Ir-192		x	x	[59]
Ir-194		x	x	[60]
Pt-195		x	x	[61], BNL/ECN
Pt-196		x	x	[62]
Pt-197		x	x	[63]
Pt-199		x	x	[63]
Au-198		x	x	[64]
Th-233		x	x	[65], BNL/ECN
U-236				[66]
U-239	x	x	x	[67,68], BNL/ECN
Pu-240		x		[14]

not present, the approximation factor of 2 has been applied, as this does not significantly influence results [21], still remaining within the statistical accuracy of the I_γ/E_γ^3 values.

Second, the calibration of the measured reduced intensities has to be performed from the comparison with DRC data using the equations

$$f(E1)_{\mathrm{ARC}} = C \times f(E1)_{\mathrm{DRC}} \tag{1}$$

and

$$f(E1)_{\mathrm{ARC}} = C \times \left(I_\gamma/E_\gamma^3\right)_{\mathrm{ARC}}. \tag{2}$$

The $E1$ transitions are primarily used because of their superior statistical accuracy and their purity (the negligible effect of p-wave contribution). The calibration against DRC $f(M1)$ values has not been used for two reasons: first the statistical accuracy is inferior to $E1$ data and second the $M1$ radiation from the capture of the 2-keV neutron beam is slightly polluted by $E1$ radiation from the p-wave capture. Therefore, the ARC $\langle f(M1)\rangle$ systematic was used only as an additional information to validate the deduced $M1$ strength.

The normalization constant C may be derived in two ways. When DRC measurements have been performed, the information can be taken either using the mean value of $f(E1)$ averaged over the transitions present in an energy range of 1 MeV, as derived in Refs. [23,69]. The advantage of this procedure is that the same transitions measured in both experiments are used. The DRC then gives the absolute transition strength.

If the DRC measurement is not available, use is made of the $\langle f(E1)\rangle$ systematic

$$\langle f(E1)\rangle = 0.0021\, A^{1.69}[10^{-8}\ \mathrm{MeV}^{-3}] \tag{3}$$

obtained on the basis of a fit to measured DRC data [70] as a function of the atomic mass A at E_γ energies around 6.2 ± 0.5 MeV. This energy dependence may form an additional uncertainty for targets in which the dominant $E1$ transitions are not in the vicinity of this energy. In such a case, the systematic value has to be adjusted assuming an additional E_γ^2 dependence. An example of such a conversion is shown in Fig. 1 for the ^{197}Au(n,γ) reaction. The detailed description of the applied conversion processing will be given in Ref. [71].

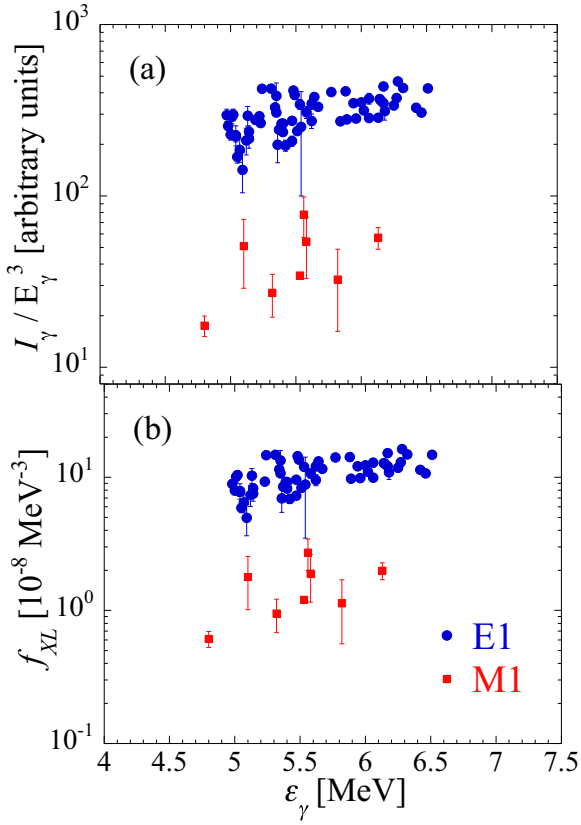

FIG. 1. (a) $E1$ and $M1$ strength in ^{198}Au from the 2 keV ARC data measured at BNL filter beam facility in I_γ/E_γ^3 arbitrary units. (b) Same after conversion into the dipole strength $f(L)$ in 10^{-8} MeV^{-3} scale, using the systematic table [64] and averaging over four $E1$ transitions.

B. Data uncertainties

1. *Statistical error of I_γ/E_γ^3*

The statistical error includes the uncertainty of the gamma ray spectrum analysis, namely the statistical accuracy and absolute intensity calibration. These errors are for moderately large and strong transitions of the order of 10–15%. However, transitions at lower γ-ray energies with a high density of γ lines or transitions with a peak intensity close to the experimental sensitivity limit may be much larger. This error is derived from the spectrum fitting and calibration treatment.

2. *Uncertainty due to the Porter-Thomas distribution*

In the extreme statistical model the gamma decay of resonant states the intensity of primary γ rays have a wide PT distribution with a χ^2 for $\nu = 1$ [72]. In a first approximation, by averaging over several resonances, the fluctuations of the partial width Γ_γ can be reduced by $\sqrt{2/\nu}$ of the relative mean-square dispersion [73] with the degrees of freedom ν equal to the number of resonances. In the application of BNL

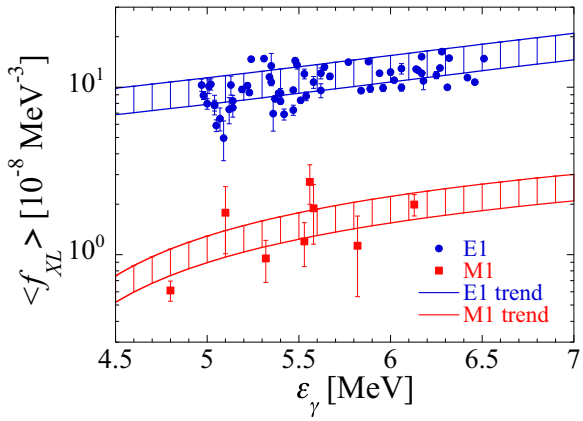

FIG. 2. (a) The PT dispersion estimated from the $\sqrt{2/\nu}$ approximation for ^{198}Au for $E1$ and $M1$ transitions. The ARC data taken from Ref. [64] measured at the BNL 2 keV filter beam facility. The general trend is depicted by the hashed area.

TABLE II. List of adopted nuclides and data sources with their calibration and ARC quantities, i.e., the mean energy E_γ of the interval of transitions used for the calibration, the mean $\langle f(E1)\rangle$ PSF (*except for ^{124}Te where it corresponds to $\langle f(M1)\rangle$) values derived from DRC or systematics (the underlined value is the one used for normalization), the $E1/M1$ ratio of the PSF in the E_γ interval from adopted data (ARC Atlas) together with the error bar, the dispersion factor dPT of the PT fluctuations derived from $\sqrt{2/\nu}$, and the estimated or calculated p-wave $E1$ contribution in $M1$ s-wave transitions. In the last estimate, the superscripts correspond to (a) RACA calculations (BNL/ECN database) (b) boron estimate, and (c) empirical estimate from this work. See text for more details.

Nucleus	n-beam	E_γ	$\langle f(E1)\rangle$		$E1/M1$		dPT	p-wave
		MeV	DRC	Sys	ARC	Err	factor	$E1$ in $M1$
			10^{-8}MeV^{-3}					
As-76	Sc [24]	6.7		2.35	3.24	1.08	0.44	0.2^c
Zr-92	Sc [75]	6.2		3.20	–	–	1.10	0.2^c
Mo-96	Sc [25]	6.6		3.43	4.51	0.44	0.43	0.66^a
Mo-98	Sc [25]	6.6		3.55	1.55	0.22	0.32	0.2^c
Ru-102	Sc [BNL/ECN]	6.8		3.78	4.26	0.55	0.20	0.33^a
Pd-106	B [8]	7.2	4.14	4.03	3.51	0.65	0.16	0^b
Cd-114	Sc [28]	6.2		4.53	2.45	0.15	0.23	0.24^a
Te-124	Sc [29]	7.1		1.44*	–	–	0.24	0.2^c
I-128	Sc [27]	6.6	(1.90)	5.47	6.36	2.33	0.15	0.2^c
Ba-135	Sc [30]	5.1		5.96	5.60	4.08	0.89	0.2^c
Ba-136	Sc [31]	6.6	5.0	6.03	5.22	0.60	0.29	0.2^c
Nd-146	B [54]	6.4	4.5	6.77	7.26	1.99	0.13	0^b
Sm-155	Sc [34]	5.4		7.46	3.33	0.40	0.50	0.21^a
Eu-154	Sc [35]	7.9		7.38	5.39	2.12	0.06	0.2^c
Gd-155	Sc [36]	5.9	9.2	7.46	3.76	1.33	0.17	0.2^c
Gd-156	B [8]	7.4		7.53	7.85	2.23	0.03	0^b
Gd-157	Sc [9]	5.9	12.4	7.61	3.36	0.29	0.26	0.15^a
Gd-158	B [40]	6.4		7.69	6.42	1.30	0.44	0^b
Gd-159	Sc [42]	5.4	8.81	7.77	3.30	0.96	0.43	0.2^c
Dy-162	Sc [43]	6.8		8.01	7.78	1.30	0.07	0.13^a
Dy-163	Sc [44]	5.7	7.26	8.09	3.76	0.42	0.37	0.2^c
Dy-164	Sc [43]	7.2		8.17	4.39	0.56	0.13	0.18^a
Dy-165	Sc [45]	5.4		8.24	2.18	0.23	0.57	0.2^c
Ho-166	B [8]	6.0		8.33	4.99	0.54	0.07	0^b
Er-168	B [8]	6.4	15.9	8.50	6.25	1.31	0.10	0^b
Tm-170	Sc [47]	6.1	(4.72)	8.66	5.12	1.38	0.17	0.2^c
Yb-172	Sc [48]	6.8		8.83	4.75	0.19	0.12	0.09^a
Yb-174	Sc [49]	6.6	19.4	8.99	4.79	0.18	0.13	0.2^c
Lu-176	Sc [51]	5.9	7.4	9.16	5.14	0.54	0.09	0.15^a
Hf-178	Sc [52]	6.8	18.5	9.33	6.25	1.41	0.07	0.2^c
Ta-182	Sc [53]	5.8	11.3	9.67	6.85	2.34	0.12	0.2^c
W-184	B [54]	6.8	28.1	9.85	7.85	1.31	0.16	0^b
W-185	Sc [55]	5.4		9.93	4.97	1.28	0.42	0.2^c
W-187	Sc [55]	5.4		10.11	3.71	0.54	0.46	0.2^c
Os-188	Sc [10]	6.3		10.20	2.77	0.72	0.10	0.2^c
Os-189	Sc [56]	5.7		10.28	3.62	0.99	0.29	0.2^c
Os-191	Sc [57]	5.4		10.46	2.94	0.26	0.39	0.2^c
Os-193	Sc [58]	5.5		10.60	–	–	0.51	0.2^c
Ir-192	Sc [59]	6.1		10.55	4.55	1.62	0.06	0.2^c
Ir-194	Sc [60]	5.9		10.73	–	–	0.09	0.2^c
Pt-195	Sc [61]	5.9		10.82	4.24	1.56	0.43	0.31^a
Pt-196	Sc [62]	6.3	17.4	10.91	–	–	0.21	0.2^c
Pt-197	Sc [63]	5.7		11.00	2.82	0.75	0.69	0.2^c
Pt-199	Sc [63]	5.3		11.18	4.80	1.12	0.87	0.2^c
Au-198	Sc [64]	6.1	11.4	11.09	5.38	1.77	0.19	0.2^c
Th-233	Sc [65]	4.1	(20.3)	14.44	4.66	1.30	0.19	0.39^a
U-239	B [67]	4.0	10.29	15.04	6.05	1.32	0.10	0^b
Pu-240	Sc [14]	5.6	19.9	15.15	4.46	0.77	0.07	0.2^c

measurements for spectroscopic purposes, this uncertainty was estimated from the Monte Carlo simulation code RACA, the details are discussed in Refs. [21,64,74]. Contrary to the spectroscopy applications, in which both 2 and 24 keV data are used to distinguish different spins and parity of final states, for PSF derivation, it is sufficient to distinguish different multipolarities of the radiation from the parity of final states. In the present experiments, the uncertainty band over the measured data points for the same multipolarity is mostly narrow enough to distinguish between $E1$ and $M1$ radiations.

The simple $\sqrt{2/\nu}$ approach is satisfactory to give a first estimate of the dispersion of the measured data. In the present analysis the $E1$, $M1$, and $E2$ data groups are clearly separated from each other by the satisfactory experimental averaging, and their multipolarity assigned prior to the analysis of the strength function. The relative variance can be estimated from the $\sqrt{2/\nu}$ factor, where ν is the number of degrees of freedom and equals to the number of resonances present in the 2-keV window. The full width at half maximum (FWHM) of the Sc filter at the BNL filtered beam facility has been determined by the transmission measurements as 0.9 keV [11]. From the beam width profile and the s-wave resonance spacing D_0 we estimate the number of resonances to be $\nu = 0.9/D_0$ leading to the PT dispersion $dPT \leqslant \sqrt{2/\nu}$. The beam profile with high neutron flux at the center and decreasing at the beam boundaries, reduces the number of effective degrees of freedom. Further, the dPT estimate may be influenced by the presence of p-wave capture, adding the contribution of the opposite multipolarity. However, it seems that despite all these effects this approximation gives sufficient information to judge the scatter (dispersion) of the data within the $E1$, $M1$, and $E2$ experimental data groups.

For illustration, the PT dispersion band for $E1$ and $M1$ transitions of the ^{197}Au(n,γ) reaction are shown in Fig. 2. The calculated trend lines were applied to guide the eye and broadened by the estimated $dPT = 1.19$ factor. It seems that the number of data points outside these bands, considering their statistical errors, is reasonable if one assumes the neutron beam profile. The resonances from the tails of the bell-shaped neutron spectrum are weak and contribute less to the averaging and thus the estimated degree of freedom is too large. However, the comparison of $\sqrt{2/\nu}$ and Monte Carlo simulation in Ref. [12] indicates that the influence is not significant. To accommodate this effect the effective FWHM of 600 eV was applied, which simulates the elimination of the weak resonances from the tails of the neutron spectrum. The corresponding effect on the degrees of freedom is shown in the last column of Table II.

For a satisfactory averaging, we only selected ARC data for nuclei with atomic mass A larger than about 70 that have enough resonances in the neutron spectrum profile. Almost all data originate from experiments with Sc filtered beam at the BNL facility. However, when boron filtered data are available, they are preferably used.

3. *Uncertainty due to p-wave E1 component in M1 radiation*

The ARC experiments use the neutron beam energies spreading from about 100 eV (B) through 2 keV (Sc) and up to 24 keV (Fe). The dominance of s-wave capture, close to thermal energies, decreases with the increasing neutron energy, so that the p-wave resonances start to contribute to the capture process. This effect has been included in the code RACA as the Monte Carlo modeling of the partial cross sections and discussed in Refs. [14,18]. In the spectroscopic application of the ARC method, the p-wave capture is primarily used for the parity determination of the final states by means of the intensity ratio of the 24 keV to the 2 keV data.

However, for PSF application, the p-wave capture both at 2 and mainly 24 keV complicates the determination of the absolute strength of $M1$ radiation, increasing the s-wave $M1$ strength by the p-wave $E1$ admixture. Contrary to that, the s-wave $E1$ capture is negligibly increased by $M1$ p-waves due the weaker $M1$ strength. The boron filtered beam with its low neutron mean energy of about 150 eV is a beam with a rather negligible p-wave component. This property was used here to introduce an empirical estimate of the average p-wave contribution based on the comparison of $E1/M1$ strength of boron and 2 kev data.

For the number of ARC data adopted in the BNL-ECN database, the $E1$ component present in $M1$ radiation was estimated by the RACA code calculations. For the remaining data, with no correction, this effect is estimated in the following way. The theoretical description of the formula for the ratio of s- and p-wave capture can be found in Refs. [12,14,18,20] and is a function of several ingredients, such as S_0, S_1, E_γ, $\Gamma_{\gamma 0}$, and $\Gamma_{\gamma 1}$. The dominant factor in this formalism (see Eq. (7) in Ref. [12]) is the S_1/S_0 ratio. We plotted the $\langle f(E1)\rangle/\langle f(M1)\rangle$ ratio against the S_1/S_0 ratio and found it most instructive to estimate the $E1$ (p-wave) component (see Fig. 3). From the trend analysis of these two boron and Sc data sets (see solid lines in Fig. 3), the mean value of the $E1$ component was estimated as 15–20%. This is a crude approach, but satisfactory to judge the $M1$ strength in comparison to the model calculations. The applied corrections to the $M1$ strength are included in Table II.

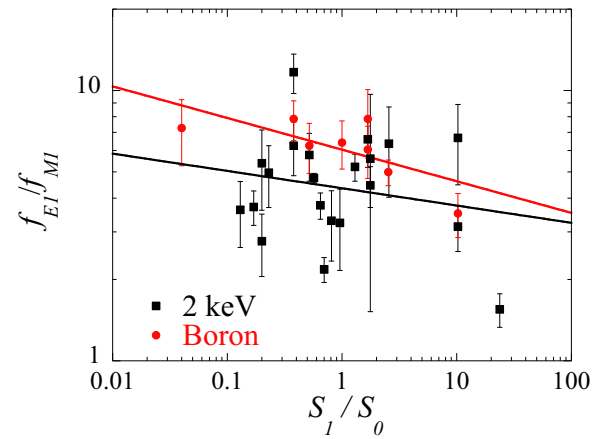

FIG. 3. Ratio of the $E1$ to $M1$ strengths extracted from ARC data as a function of the ratio S_1/S_0. The black squares correspond to the 2-keV data and the red circles to the boron data. The general trends in both cases are shown by the regression solid lines.

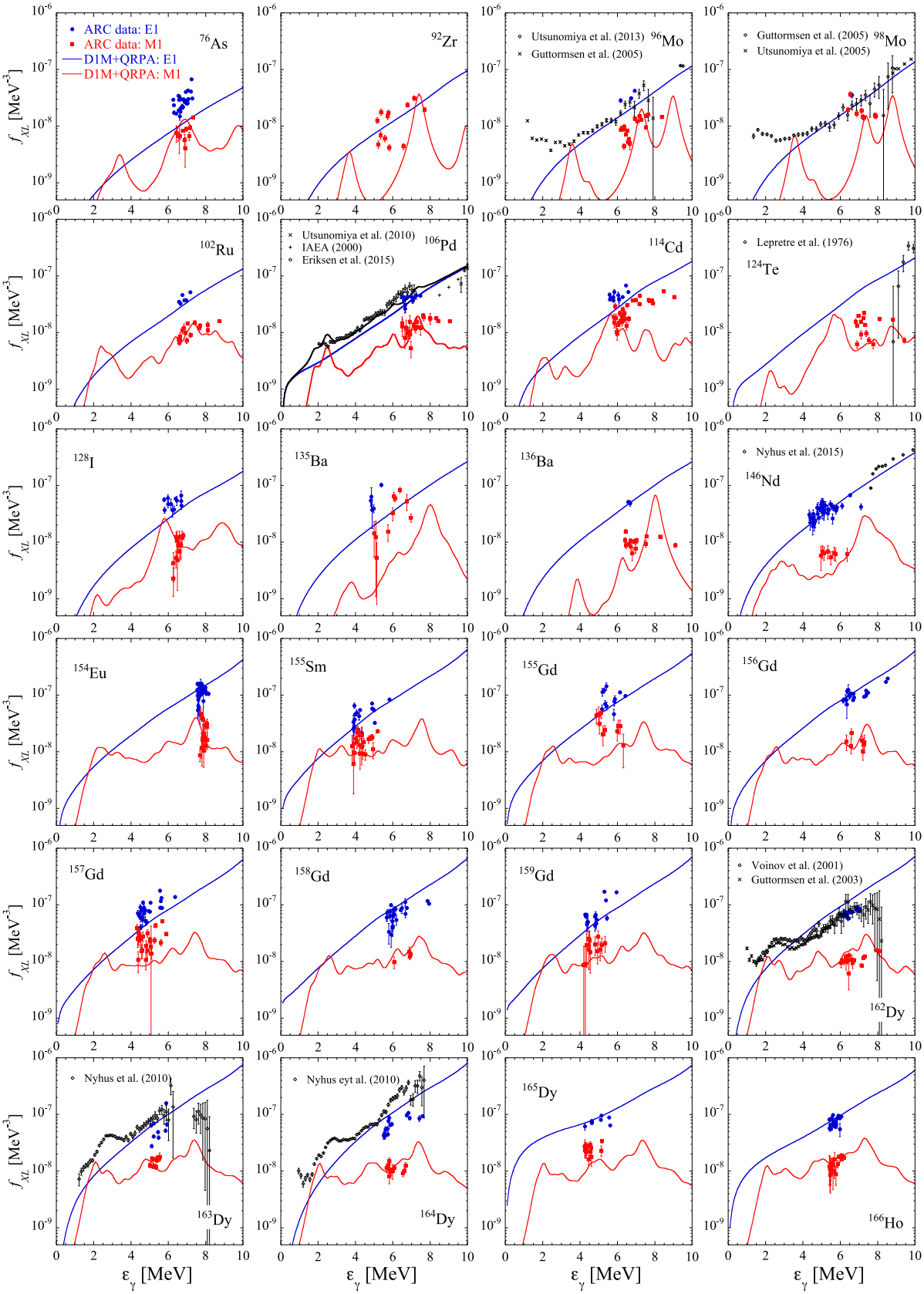

FIG. 4. Comparison between $E1$ and $M1$ strength functions derived from ARC data and D1M + QRPA calculations [76,77]. Also shown are the total strength functions extracted from other measurements, in particular (γ,n) cross section or transfer reaction through the Oslo method, for ^{96}Mo [78,79], ^{106}Pd [80–82], ^{124}Te [83], ^{146}Nd [84], ^{162}Dy [85,86], $^{163-164}$Dy [87].

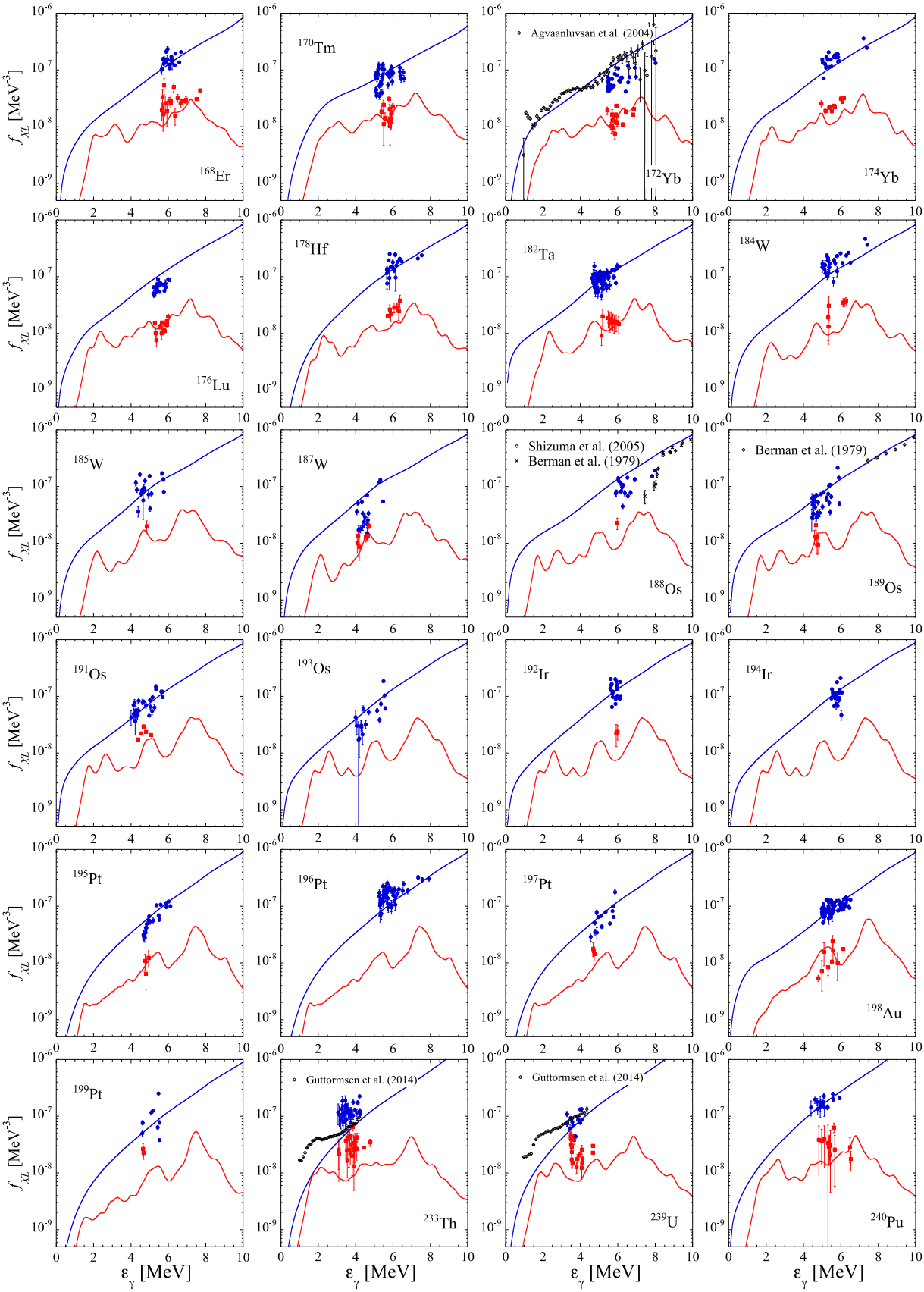

FIG. 5. Same as Fig. 4. Experimental strengths are taken from [88] for ^{172}Yb, [89] for ^{188}Os, [90] for ^{189}Os, and from [91] for ^{233}Th and ^{239}U.

C. Summary of ARC data

All ARC data reviewed and selected as final data sources in this work are listed in Table II and will be available in the near future as an INDC report [71]. The 2-keV spectra are preferably used due their purity and statistical and averaging quality. Similarly, all boron filter beam measurements are preferentially considered, because their p-wave component is negligible and the $E1/M1$ ratio is a clean experimental quantity. The boron beam profile spreads asymmetrically from 10 up to 2000 eV, with the maximum around 150 eV. The FWHM value of 2000 eV is used for the estimate of the PT dispersion.

The ARC database consists for each nucleus of a data file with I_γ/E_γ^3 data, extracted from quoted references, and the strength function $f(L)$ file in 10^{-8} MeV^{-3} units. The uncertainty of the $f(L)$ values are purely of statistical origin. The normalization factor is taken from the table of averaged $E1$ strength $\langle f(E1)\rangle$ derived from the DRC experiments averaged over the number of resonances and primary transitions [70]. For nuclides without DRC data and missing in the table, the systematic equation [Eq. (3)] for $\langle f(E1)\rangle$ is used instead, for details see Ref. [70].

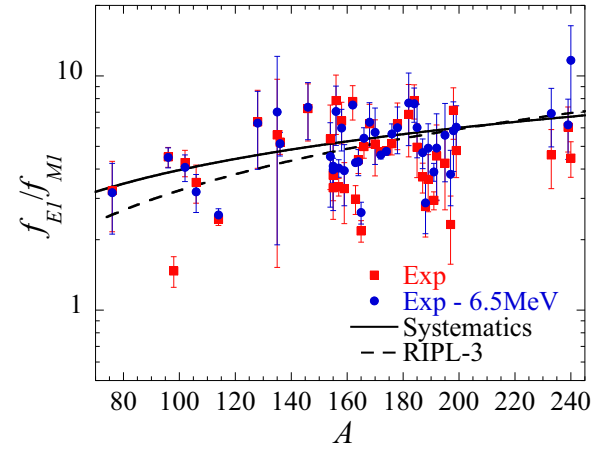

FIG. 6. Ratio of the $E1$ to $M1$ strengths extracted from ARC data as a function of the atomic mass A. The read squares correspond to the ratio at the measured average energy and the blue circles to data renormalized at 6.5 MeV. The solid line is the newly proposed systematics of $f_{E1}/f_{M1} = 0.25A^{0.6}$ at 6.5 MeV. The dashed line is the widely used RIPL-3 systematics $f_{E1}/f_{M1} = 0.059A^{0.87}$ [23,92].

III. COMPARISON TO OTHER DATA AND QRPA CALCULATIONS

The ARC data presented in Sec. II are now compared to other experimental results and with theoretical predictions. Recently, axially-symmetric-deformed quasiparticle random phase approximation (QRPA) estimates based on Hartree-Fock-Bogoliubov (HFB) calculations using the finite-range D1M Gogny interaction have been shown to provide rather satisfactory predictions of the $E1$ [76] and $M1$ [77] strength functions. We compare here the ARC $E1$ and $M1$ strength functions to the D1M + QRPA calculation and at the same occasion with other experimental determinations, including, in particular, photonuclear data or the transfer reaction through the so-called Oslo method. It should, however, be kept in mind that photonuclear data at low energies correspond to (γ,n) measurements from which it remains difficult to extract information on the PSF in the vicinity of the neutron separation energy. Such photodata are also only available for stable targets. Both photonuclear data and the Oslo data refer to the total (i.e., essentially $E1 + M1$) photon strength, so we could expect the corresponding data, especially in the case of the Oslo method, to be slightly higher than those evaluated from ARC measurements. Globally, as shown in Figs. 4 and 5, the agreement between the newly evaluated ARC data and former measurements is rather good although some deviations can be seen for some nuclei like ^{135}Ba and the actinides ^{233}Th and ^{239}U. The presence of the fission channel leads to different behaviors in resonance averaging, as discussed for ^{240}Pu in Ref. [14]. It was, however, not accounted for in the ^{233}Th and ^{239}U analysis.

We compare in Figs. 4 and 5 the $E1$ and $M1$ strengths derived from ARC data with those obtained within the D1M + QRPA approach [76,77]. Most of the nuclei for which ARC data are available correspond to deformed nuclei, except for light nuclei like ^{76}As, ^{92}Zr, ^{96,98}Mo, or ^{135,136}Ba, as seen by the $M1$ strength pattern from QRPA predictions. Indeed, for deformed nuclei QRPA calculations give an additional low-energy component corresponding to the scissors mode which is absent in spherical nuclei where the spin-flip resonance dominates around 8–10 MeV [77]. In general, the agreement between D1M + QRPA and $E1$ and $M1$ ARC data is rather satisfactory, despite some outliers for the $M1$ strength, including some species like ^{157}Gd and the above-mentioned actinides where D1M + QRPA underestimates the $E1$ and $M1$ ARC data. Some of the disagreements may also be due to the uncertain conversion between I_γ/E_γ^3 into the PSF which remains affected by the uncertain DRC evaluations old of some 30 to 40 years.

While both the $E1$ and $M1$ strengths are affected by uncertainties, as described in Sec. II B, the ratio of the $E1$ to $M1$ strengths remains independent from the conversion procedure from the intensities I_γ/E_γ^3 into a PSF, if the competing $E1$ contribution to $M1$ transitions for the p-wave capture is properly taken care of (see Sec. II B 3). We show in Fig. 6 the $E1$-to-$M1$ ratio as a function of the atomic mass A, both from the original ARC data at energies ranging between 3.6 and 7.2 MeV and after renormalizing the ARC data at the average reference energy of 6.50 ± 0.25 MeV. The energy regions of $E1$ and $M1$ data (on average about 1 MeV broad) were chosen identical to minimize the internal energy dependence between them. For the renormalization to the reference energy, an empirical factor, derived from the present ARC data, was applied. As can be seen in Fig. 6, the original $E1/M1$ ratio is widely distributed between 1.5 and 7.8. However, this ratio is obtained at different energies and for nuclei that can be either spherical or deformed. It is therefore not recommended to extract some systematics from such data.

Previous analyses of ARC data [70,92] led to some systematics at the reference energy of 6.2 MeV; more precisely

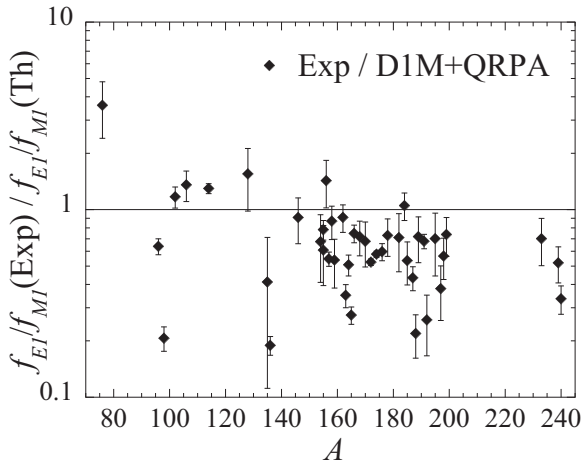

FIG. 7. Comparison of the ratio of the $E1$ to $M1$ strengths extracted from ARC data with the one obtained within the D1M + QRPA framework as a function of the atomic mass A.

it was proposed to consider the $f_{E1}/f_{M1} = 0.059A^{0.87}$ trend. This expression is the one recommended by the RIPL-3 library at the reference energy of 7 MeV [23]. With the additional data available now, we can further test and improve this systematics. As shown in Fig. 6, at the reference energy of 6.5 MeV, an average ratio of $f_{E1}/f_{M1} = 0.25A^{0.6}$ can explain the general trend. This agreement supports the compatibility of DRC and ARC measurements. However, a large dispersion around such a systematics is also found, so that it remains hazardous to use such expressions for single events and not as a trend only.

Finally, we compare in Fig. 7 the ratio of the $E1$ to $M1$ strengths extracted from ARC data with the one obtained within the D1M + QRPA framework. The D1M + QRPA $E1$ and $M1$ strengths have been averaged over the energy range corresponding to the ARC measurement. While the calculated ratio is globally in rather good agreement with ARC data, the QRPA calculation tends to overestimate by some 20% the ratio, either by overestimating the $E1$ strength or, most systematically as seen in Figs. 4 and 5, underestimating the $M1$ strength. Such a comparison between the ARC and theoretical $E1$-to-$M1$ strength ratio is a stringent test for the elaboration of future models for the dipole strength function.

IV. CONCLUSION

ARC data measured at different filter beam facilities have been reanalyzed. They include all measurements made at ANL, INEL, and BNL between 1970 and 1990, but only partially exploited. This is the first time that a comprehensive re-evaluation of all measured data was completed and applied for a systematic comparison with estimated PSF. Updated spectroscopic information on the states of interest is used to extract the $E1$ and $M1$ PSF. This re-evaluation provides new experimental information on the $E1$ and $M1$ strength function around the neutron binding energy and doing so also provides new constraints for existing γ-ray strength models used in statistical reaction codes. Globally, the revised data agree rather well with the total strength function extracted from photoneutron data or from transfer or inelastic reactions by the so-called Oslo method. The ARC data also show that the recent QRPA calculations based on the D1M Gogny force give rather satisfactory predictions, both for the $E1$ and $M1$ strengths. The ratio of the $E1$ to $M1$ strength functions is found to remain within the small range of 1.5 and 7.8 but not to follow any clear systematics, as expected from microscopic predictions. The ARC $E1$-to-$M1$ strength ratio represents a new stringent test for the future elaboration of theoretical models for the dipole strength function.

ACKNOWLEDGMENTS

JK acknowledges the long and fruitful collaboration with the late R. E. Chrien. We acknowledge PRACE for awarding us access to resource CURIE based in FRANCE at TGCC-CEA. SG acknowledges the support of the FRS-FNRS. This work was performed within the IAEA CRP on Updating the Photonuclear data Library and generating a Reference Database for Photon Strength Functions (F410 32).

[1] R. Schwengner, R. Beyer, F. Dönau, E. Grosse, A. Hartmann, A. Junghans, S. Mallion, G. Rusev, K. Schilling, W. Schulze, and A. Wagner, Nucl. Instr. Meth. A **555**, 211 (2005).
[2] A. P. Tonchev, S. L. Hammond, J. H. Kelley, E. Kwan, H. Lenske, G. Rusev, W. Tornow, and N. Tsoneva, Phys. Rev. Lett. **104**, 072501 (2010).
[3] A. Schiller, L. Bergholt, M. Guttormsen, E. Melby, J. Rekstad, and S. Siem, Nucl. Instrum. Methods A **447**, 498 (2000).
[4] J. Kroll *et al.*, Phys. Rev. C **88**, 034317 (2013).
[5] P. Carlos, H. Beil, R. Bergere, A. Lepretre, and A. Veyssiere, Nucl. Phys. A **172**, 437 (1971).
[6] S. S. Dietrich and B. L. Berman, At. Data Nucl. Data Tables **38**, 199 (1988).
[7] P. Dimitriou, R. Firestone, and S. Siem, *Compilation and Evaluation of Gamma-Ray Data*, IAEA Tech. Rep., INDC(NDS)-0649 (2013).
[8] L. M. Bollinger and G. E. Thomas, Phys. Rev. C **2**, 1951 (1970).
[9] R. Greenwood and C. Reich, Nucl. Phys. A **223**, 66 (1974).
[10] A. Murzin *et al.*, in Proc. of the 40th Ann. Conf. Nucl. Structure At. Nuclei (Leningrad 1990), unpublished.
[11] R. Greenwood and R. Chrien, Nucl. Instrum. Methods **138**, 125 (1976).
[12] J. Kopecky, *Capture Gamma-Ray Spectroscopy and Related Topics* (American Institute of Physics, New York, 1985), p. 318.
[13] R. F. Casten, D. D. Warner, M. L. Stelts, and W. F. Davidson, Phys. Rev. Lett. **45**, 1077 (1980).
[14] R. Chrien, J. Kopecky, H. Liou, O. Wasson, J. Garg, and M. Dritsa, Nucl. Phys. A **436**, 205 (1985).
[15] J. Kopecky and R. Chrien, Nucl. Phys. A **468**, 285 (1987).
[16] J. Kopecky and M. Uhl, Phys. Rev. C **41**, 1941 (1990).
[17] J. Kopecky, M. Uhl, and R. E. Chrien, Phys. Rev. C **47**, 312 (1993).

[18] R. Chrien, *Neutron Gamma Ray Spectroscopy and Related Topics* (Institute of Physics, Bristol, England, 1982), Vol. 62, p. 342.
[19] R. Chrien, in *Fourth Int. Symposium on Neutron Induced Reactions*, edited by J. Kristiak, E. Betak, and D. Reidel (Smolenice, 1985), p. 200.
[20] M. Stelts, Nat. Bur. Stds. Sp. Pub. **594**, 936 (1980).
[21] R. Chrien, Phys. Conf. Ser. **62**, 342 (1981).
[22] S. Mughabghab, *Atlas of Neutron Resonances* (Elsevier, Amsterdam, 2006).
[23] R. Capote *et al.*, Nucl. Data Sheets **110**, 3107 (2009).
[24] F. Hoyler *et al.*, Nucl. Phys. A **512**, 189 (1990).
[25] A. F. Gamalii *et al.*, Sov. J. Nucl. Phys **15**, 1 (1972).
[26] B. Fogelberg *et al.*, Nucl. Phys. A **475**, 301 (1987).
[27] C. M. McCullagh, Ph.D. Thesis, Department of Physics, State University of New York at Stony Brook, 1978.
[28] A. Meemeed *et al.*, Nucl. Phys. A **412**, 113 (1984).
[29] R. F. Casten, J.-Y. Zhang, and B.-C. Liao, Phys. Rev. C **44**, 523 (1991).
[30] R. E. Chrien, B. K. S. Koene, M. L. Stelts, R. A. Meyer, S. Brant, V. Paar, and V. Lopac, Phys. Rev. C **48**, 109 (1993).
[31] K. Schreckenbach *et al.*, Phys. Conf. Ser. **62**, 200 (1981).
[32] D. L. Bushnell, G. R. Tassotto, and R. Smither, Phys. Rev. C **14**, 75 (1976).
[33] S. Raman, J. Phys. G: Nucl. Part. Phys. **9**, L137 (1983).
[34] K. Schreckenbach *et al.*, Nucl. Phys. A **376**, 149 (1982).
[35] M. K. Balodis *et al.*, Nucl. Phys. A **472**, 445 (1987).
[36] H. Schmidt *et al.*, J. Phys. G: Nucl. Part. Phys. **12**, 411 (1986).
[37] R. C. Greenwood *et al.*, Proceedings of Neutron Gamma Ray Capture Spectroscopy and related topics (1974).
[38] R. C. Greenwood and R. Chrien, Bull. Am. Phys. Soc. 8, ED9 **22**, 1032 (1977).
[39] A. Bäcklin *et al.*, Nucl. Phys. A **380**, 189 (1982).
[40] R. Greenwood, C. Reich, H. Baader, H. Koch, D. Breitig, O. Schult, B. Fogelberg, A. Bäcklin, W. Mampe, T. V. Egidy, and K. Schreckenbach, Nucl. Phys. A **304**, 327 (1978).
[41] T. D. MacMahon, G. R. Massoumi, T. Mitsunari, M. Thein, O. Chalhoub, D. Breitig, H. A. Baader, U. Heim, H. R. Koch, and L. Wimmer, J. Phys. G **11**, 1231 (1985).
[42] C. Granja, S. Pospíšil, S. Telezhnikov, and R. Chrien, Nucl. Phys. A **729**, 679 (2003).
[43] D. D. Warner, R. F. Casten, W. R. Kane, and W. Gelletly, Phys. Rev. C **27**, 2292 (1983).
[44] H. Schmidt *et al.*, Nucl. Phys. A **504**, 1 (1989).
[45] E. Kaerts *et al.*, Nucl. Phys. A **514**, 173 (1990).
[46] W. Davidson, D. D. Warner, R. Casten, K. Schreckenbach, H. Borner, J. Simic, M. Stojanovic, M. Bogdanovic, S. Koicki, and W. Gelletly, J. Phys. G **7**, 843 (1981).
[47] R. W. Hoff, H. G. Borner, K. Schreckenbach, G. G. Colvin, F. Hoyler, W. Schauer, T. vonEgidy, R. Georgii, J. Ott, S. Schrunder, R. F. Casten, R. L. Gill, M. Balodis, P. Prokofjevs, L. Simonova, J. Kern, V. A. Khitrov, A. M. Sukhovoj, O. Bersillon, S. Joly, G. Graw, D. Hofer, and B. Valnion, Phys. Rev. C **54**, 78 (1996).
[48] R. Greenwood, C. W. Reich, and S. H. Vegors Jr., Nucl. Phys. A **252**, 260 (1975).
[49] C. Granja, S. Pospíšil, R. Chrien, and S. Telezhnikov, Nucl. Phys. A **757**, 287 (2005).
[50] R. C. Greenwood and C. W. Reich, Phys. Rev. C **23**, 153 (1981).
[51] R. Hoff, R. Casten, M. Bergoffen, and D. Warner, Nucl. Phys. A **437**, 285 (1985).
[52] A. Hague, R. Casten, I. Förster, A. Gelberg, R. Rascher, R. Richter, P. V. Brentano, G. Berreau, H. Börner, S. Kerr, K. Schreckenbach, and D. Warner, Nucl. Phys. A **455**, 231 (1986).
[53] R. Helmers *et al.*, Nucl. Phys. A **168**, 449 (1971).
[54] D. Bushnell, Phys. Rev. C **11**, 1401 (1975).
[55] A. Bruce *et al.*, Nucl. Phys. A **465**, 221 (1987).
[56] A. Bruce, Nucl. Phys. A **542**, 1 (1992).
[57] R. Casten *et al.*, Nucl. Phys. A **285**, 235 (1977).
[58] D. Warner, W. Davidson, H. Börner, R. Casten, and A. Namenson, Nucl. Phys. A **316**, 13 (1979).
[59] J. Kern, Nucl. Phys. A **534**, 77 (1991).
[60] M. Balodis *et al.*, Nucl. Phys. A **641**, 133 (1998).
[61] D. D. Warner, R. F. Casten, M. L. Stelts, H. G. Börner, and G. Barreau, Phys. Rev. C **26**, 1921 (1982).
[62] J. Cizewski *et al.*, Nucl. Phys. A **323**, 349 (1979).
[63] R. F. Casten, D. D. Warner, G. M. Gowdy, N. Rofail, and K. P. Lieb, Phys. Rev. C **27**, 1310 (1983).
[64] U. Mayerhofer *et al.*, Nucl. Phys. A **492**, 1 (1989).
[65] P. Jeuch *et al.*, Nucl. Phys. A **317**, 363 (1979).
[66] H. Ottmar *et al.*, Proc. Int. Symposium on Neutron Capture Gamma-rays Spectroscopy and related Topics p. 658 (1974).
[67] L. M. Bollinger and G. E. Thomas, Phys. Rev. C **6**, 1322 (1972).
[68] R. Chrien and J. Kopecky, Nucl. Phys. A **414**, 281 (1984).
[69] C. M. McCullagh, M. L. Stelts, and R. E. Chrien, Phys. Rev. C **23**, 1394 (1981).
[70] J. Kopecky, Present Status of Experimental Gamma-Ray Strength Functions derived from Neutron Capture, INDC(NED)-13 (2016).
[71] J. Kopecky, Atlas of Average Resonance Capture Data, INDC(NED) Report (to be published, 2017).
[72] C. Porter and R. Thomas, Phys. Rev. **104**, 483 (1956).
[73] L. Bollinger and G. Thomas, in *Slow Neutron Capture Gamma-ray Spectroscopy* (Argone National Laboratory, Argone, IL, 1968).
[74] F. Becvar, Private Communication (2016).
[75] M. Kenny *et al.*, in *Proceedings of Neutron Gamma Ray Capture Spectroscopy and Related Topics* (Upton, El Segundo, CA, 1978), p. 676.
[76] M. Martini, S. Péru, S. Hilaire, S. Goriely, and F. Lechaftois, Phys. Rev. C **94**, 014304 (2016).
[77] S. Goriely, S. Hilaire, S. Péru, M. Martini, I. Deloncle, and F. Lechaftois, Phys. Rev. C **94**, 044306 (2016).
[78] H. Utsunomiya *et al.*, Phys. Rev. C **88**, 015805 (2013).
[79] M. Guttormsen *et al.*, Phys. Rev. C **71**, 044307 (2005).
[80] H. Utsunomiya *et al.*, Phys. Rev. C **82**, 064610 (2010).
[81] *Handbook on Photonuclear Data for Applications*, Tech. Rep., IAEA TECDOC- 1178 (2000).
[82] T. K. Eriksen, H. T. Nyhus, M. Guttormsen, A. Görgen, A. C. Larsen, T. Renstrøm, I. E. Ruud, S. Siem, H. K. Toft, G. M. Tveten, and J. N. Wilson, Phys. Rev. C **90**, 044311 (2014).
[83] A. Lepretre, H. Beil, R. Bergére, P. Carlos, J. Fagot, A. D. Miniac, A. Veyssiére, and H. Miyase, Nucl. Phys. A **258**, 350 (1976).
[84] H.-T. Nyhus *et al.*, Phys. Rev. C **91**, 015808 (2015).
[85] A. Voinov, M. Guttormsen, E. Melby, J. Rekstad, A. Schiller, and S. Siem, Phys. Rev. C **63**, 044313 (2001).

[86] M. Guttormsen, A. Bagheri, R. Chankova, J. Rekstad, S. Siem, A. Schiller, and A. Voinov, Phys. Rev. C **68**, 064306 (2003).

[87] H. T. Nyhus, S. Siem, M. Guttormsen, A. C. Larsen, A. Bürger, N. U. H. Syed, G. M. Tveten, and A. Voinov, Phys. Rev. C **81**, 024325 (2010).

[88] U. Agvaanluvsan, A. Schiller, J. A. Becker, L. A. Bernstein, P. E. Garrett, M. Guttormsen, G. E. Mitchell, J. Rekstad, S. Siem, A. Voinov, and W. Younes, Phys. Rev. C **70**, 054611 (2004).

[89] T. Shizuma, H. Utsunomiya, P. Mohr, T. Hayakawa, S. Goko, A. Makinaga, H. Akimune, T. Yamagata, M. Ohta, H. Ohgaki, Y. W. Lui, H. Toyokawa, A. Uritani, and S. Goriely, Phys. Rev. C **72**, 025808 (2005).

[90] B. L. Berman, D. D. Faul, R. A. Alvarez, P. Meyer, and D. L. Olson, Phys. Rev. C **19**, 1205 (1979).

[91] M. Guttormsen *et al.*, Phys. Rev. C **89**, 014302 (2014).

[92] J. Kopecky, *ECN-RX-92-011*, Technical Report No. 011, ECN (1992).